Available online at www.sciencedirect.com
SCIENCE DIRECT
Polymer 46 (2005) 383–396
polymer
www.elsevier.com/locate/polymer

Confined crystallization phenomena in immiscible polymer blends with dispersed micro- and nanometer sized PA6 droplets, part 2: reactively compatibilized PS/PA6 and (PPE/PS)/PA6 blends

R.T. Tol, V.B.F. Mathot, G. Groeninckx*

Laboratory for Macromolecular Structural Chemistry, Department of Chemistry, Catholic University of Leuven, Celestijnenlaan 200F, B-3001, Heverlee, Belgium

Received 3 April 2004; received in revised form 11 October 2004; accepted 20 October 2004
Available online 13 November 2004

Abstract

In this paper the relation between the blend phase morphology and the fractionated crystallization behavior of PA6 in reactively compatibilized immiscible PS/PA6 and (PPE/PS)/PA6 immiscible blends is studied. Reactive compatibilization is used as an effective tool for controlling the blend phase morphology, and to reduce the PA6 dispersed droplet size. As reactive compatibilizers, SMA2 and SMA17 are used, which differ in their level of miscibility with the amorphous PS and (PPE/PS) components. With SMA2 a strong shift of PA6 crystallization to much higher supercoolings than before is found after compatibilization resulting in crystallization at temperatures as low as 85 °C. This is ascribed to the strong decrease of the droplet sizes down to 100–150 nm. Nucleation experiments show that heterogeneous bulk nucleation can be reintroduced in the submicron-sized PA6 droplets by adding enough nucleating agents of sufficient small size. The degree of fractionated crystallization is found to depend on the interface between PA6 droplets and surrounding medium, as it is influenced by vitrification of the matrix polymer and by the location of the compatibilizers SMA2 and SMA17. The method used for mixing the reactive compatibilizer with the blend components also affects the fractionated crystallization process.

Keywords: Droplet crystallization; Blend morphology; Reactive compatibilization

1. Introduction

Crystallization of semicrystalline polymers usually takes place via heterogeneous nucleation, because of the large amount of impurities (catalyst residues etc.) that act as substrates for nucleation. However, in case of polymers dispersed as small droplets in a solvent, strong changes in crystallization behavior have been observed [1–5]. Cormia et al. and Koutksy et al. [1,2] reported on the homogeneous nucleation, taking place in small crystallizable droplets at very high supercoolings. It was ascribed to the increased probability of obtaining isolated and heterogeneity-free droplets, when the number of droplets per unit volume is strongly increased upon dispersing them.

Similar observations were made for crystallizable blocks in micro-phase separated block copolymers by Lotz et al. [6], O'Malley et al. [7] and Rubitaille et al. [8]. In these systems, besides a crystallization peak in the normal temperature range, a crystallization peak was also found at lower temperatures, which was ascribed to the crystallization in the confined domains. In a number of recent studies on micro-phase separated di- and tri-block copolymers, the effect of confinement to nanometer scale domains ($\sim$10–30 nm) on the crystallization behavior has been investigated. The observed low temperature crystallization peak is attributed to homogeneous nucleation induced at high supercoolings [9–15]. Müller et al. recently showed that the lack of active nuclei in the confined block copolymer domains plays a major role in the occurrence of homogeneous nucleation [13].

For immiscible polymer blends, where a semicrystalline component is dispersed as small droplets inside another

* Corresponding author. Tel.: +32 1 632 7440; fax: +32 16 32 7990.
E-mail address: gabriel.groeninckx@chem.kuleuven.ac.be (G. Groeninckx).

0032-3861/$ - see front matter © 2004 Elsevier Ltd. All rights reserved.
doi:10.1016/j.polymer.2004.10.070

polymer matrix, similar behavior to the droplet experiments was found. The relation between the obtained blend morphology and crystallization behavior was clearly demonstrated for many different blend systems (See Refs. [16–21] for representative papers and reviews). When the droplet size is small enough and the number of droplets per unit volume dispersed in the matrix exceeds the number of nuclei active at $T_{c,bulk}$, crystallization usually takes place in different steps, at increasing supercoolings, via nucleation by various types of heterogeneities that require larger supercoolings to become active. In several cases, massive crystallization at a quite low temperature is observed, which is ascribed to be related to homogeneous nucleation in heterogeneity-free droplets.

Reactive compatibilization of immiscible polymer blends is a widely used technique for controlling the phase morphology of the blend. Efficient compatibilization will lead to a strong reduction in dispersed droplet size, an improved stability of the droplets and an increased interfacial adhesion between the phases, strongly improving the final (mechanical and thermal) properties of the blend. This technique forms an interesting approach for investigating the homogeneous nucleation and fractionated crystallization phenomena by decreasing the size of the droplets into the sub-micrometer range. The compatibilizer formed at the interface of the two blend components, however, can be expected to influence the crystallization behavior within the droplets. Earlier reports on polymer nucleation and crystallization stress the importance of the interface in both immiscible polymer blends (matrix/droplet interface) [19,21,22–24] or in the 'droplet' experiments (droplet/medium interface) [3,5].

The number of fundamental studies investigating the effect of compatibilization on the droplet crystallization phenomena is limited and mostly only qualitatively relates addition of the compatibilizer to the decreased droplet size [18,25–30]. Recently, a more quantitative study has been performed by Pompe et al. [31] on reactively compatibilized PA/PP blends. A study by Ikkala et al. [25] indicates that the crystallization of PP droplets dispersed in a PA6 matrix can clearly be affected by the type and miscibility of the compatibilizer used. Compatibilizers forming an immiscible interlayer between both blend components were found to prevent nucleation phenomena from one component to the other. The aim of this study is to establish relations between the crystallization behavior, blend phase morphology and presence of the compatibilizer at the interface, in case of finely dispersed droplets in immiscible blends after compatibilization. For this purpose, PS/PA6 and (PPE/PS)/PA6 blend systems are used, to which two different types of reactive compatibilizer SMA are added, differing in their level of miscibility with the blend components PS and (PPE/PS). The effect of the concentration of the compatibilizers and the way of preparing the blends on the droplet crystallization is investigated too. Finally, the effect of the nucleation density on the PA6 droplet crystallization is investigated by performing various nucleation experiments.

2. Materials and methods

2.1. Materials

The polymers used in this study are listed in Table 1, together with M_w and T_g. Polyamide-6 (PA Akulon K123) was provided by DSM Research, Geleen, The Netherlands. Atactic polystyrene (PS Styron E680) was supplied by DOW Benelux, Terneuzen, The Netherlands. Poly (2,6-dimethyl-1,4-phenelyne ether) (PPE) was supplied General Electric Plastics, Bergen op Zoom, The Netherlands. The miscible polystyrene/polyphenylene-ether (PPE/PS) 50/50 w/w mixture was prepared by mixing PPE and PS in a Haake Rheocord 90 twin-screw extruder [31]. PPE and PS have different glass transition temperatures, but show equal surface tensions [31]. Styrene-maleic anhydride copolymers SMA2 (SEA 0579) and SMA17 (KCO 0950) were provided by Bayer, Dormagen, Germany. The number after SMA denotes the wt% maleic anhydride in SMA. Talc powder was kindly provided by DSM Research, Geleen, The Netherlands.

2.2. Blend preparation

The blends were prepared on a co-rotating twin-screw mini-extruder manufactured by DSM Research. Before processing, all materials were dried overnight under vacuum at 80 °C. To be able to investigate the effect of the compatibilization reaction of the reactive compatibilizers SMA2 or SMA17 with PA6 on the crystallization behavior of PA6, a number of binary PA6/SMA2 and PA6/SMA17 mixtures were prepared, with varying PA6/SMA ratio. These binary blends were melt-mixed at 240 °C during 4 min. Two different mixing methods were applied for preparation of the ternary reactive compatibilized blends. In mixing method 1, SMA2 or SMA17 were premixed with PS or (PPE/PS 50/50 w/w), in the first step at 260 °C during 8 min. In the second blending step this mixture was blended with PA6. In mixing method 2, the prepared binary blends of PA6/SMA2 and PA6/SMA17 were blended with either PS or (PPE/PS 50/50) in a second blending step. All blends were mixed at 260 °C for 8 min at a screw speed of 100 rpm in the second blending step. During melt-blending the

Table 1
Molecular characteristics of the blend components used

Materials	M_w (g mol^{-1})	T_g (DSC) (°C)
PS	190,000	102
(PPE/PS) 50/50 w/w	54,300/190,000	150
PA6	24,000	50
SMA2	120,000	105
SMA17	210,000	130

mixing chamber was saturated with N_2 gas to avoid oxidative degradation. After mixing, the blends were quenched in a mixture of CO_2/isopropanol (−78 °C) in order to freeze the existing phase morphology. PS and PPE are known to be miscible with SMA, up to MA content of about 3 wt% for PS and up to 8 wt% for PPE [32,33]. To determine the level of miscibility of (PPE/PS 50/50 w/w) and SMA17, a binary blend of (PPE/PS) and SMA17 in a weight ratio of 50/50 was prepared. A number of blends was also prepared with talc powder as nucleating agent, which was premixed with PA6 during 4 minutes at 240 °C in concentrations of 0.5 or 2 wt% prior to blending with the matrix components PS or PS/SMA2.

2.3. Morphological characterization via dissolution experiments and SEM

The morphology of the extruded blends was analyzed by means of dissolution experiments. Dissolution experiments were performed to determine if the prepared blend was a droplet/matrix or a co-continuous morphology. A small piece of the sample (about 0.025 cm^3) was immersed in formic acid at room temperature. Formic acid is a solvent for PA6 and a non-solvent for PS, (PPE/PS 50/50), PPE and SMA2. A second piece was put in chloroform at room temperature. Chloroform is a solvent for PS, (PPE/PS 50/50), PPE and SMA2 and a non-solvent for PA6. The complete procedure was repeated twice. With a droplet/matrix morphology, a solvent dissolving the matrix would cause disintegration of the sample, resulting in a milky suspension. The solvent for the droplet phase will just extract that phase, leaving the matrix intact. In a co-continuous system, neither of the solvents would cause a complete disintegration of the blend. For a complete description of the procedure and a detailed overview of the morphology development in the compatibilized PS/PA6 and (PPE/PS)/PA6 blends see Ref. [34].

The morphology of the blends has been characterized by scanning electron microscopy (SEM) on a Philips XL20 using an accelerating voltage of 20 kV. An extruded polymer strand was first broken in liquid nitrogen to obtain a fracture surface perpendicular to the extrusion direction. A Leica Ultracut UCT cryo-microtome, equipped with a Leica EM FCS cryo unit, at a sample temperature of −100 °C was used to smoothen the fractured surface. Subsequently, the samples were exposed to either formic acid or to chloroform (16 h and 40 h, respectively) to remove one phase. The etched surface was dried under vacuum and then coated with a conductive gold layer before SEM analysis. The SEM photographs used for image analysis (Section 2.4) were obtained after subjecting the samples to the same thermal program as used in dynamic crystallization experiments with DSC (Section 2.5).

2.4. Image analysis

Image analysis on the obtained SEM micrographs was performed using Leica Qwin image analysis software. For the systems with a droplet/matrix structure, the average sizes and the size distribution of the dispersed droplets were determined. About six SEM photographs (each containing about 150–300) droplets) were analyzed for each blend. The number average droplet diameter (D_n), volume average diameter (D_v) and the polydispersity (P) were calculated from:

$$D_n = \frac{\sum_i n_i d_i}{\sum_i n_i} \quad (1)$$

$$D_v = \frac{\sum_i n_i d_i^4}{\sum_i n_i d_i^3} \quad (2)$$

Polydispersity: $P = D_v/D_n$

with n_i the number of droplets having diameter d_i.

The characteristic diameters are given as seen in SEM and were not corrected for the fact that not all droplets were cut at their largest cross-section. The total number of droplets per unit volume (dispersed) polymer was calculated from:

$$N_n = \frac{X}{(\pi/6(D_n)^3)} \quad (3)$$

$$N_v = \frac{X}{(\pi/6(D_v)^3)} \quad (4)$$

with: N_n: total number of droplets per unit volume based on D_n, N_v: total number of droplets per unit volume based on D_v, X: volume fraction of dispersed phase in the blend.

2.5. Thermal analysis

2.5.1. Dynamic and isothermal crystallization experiments

Dynamic and isothermal DSC measurements were performed using a Perkin Elmer Pyris 1. The nitrogen flow-rate was 20 ml/min. Temperature and enthalpy calibrations were performed with indium (T_m = 156.6 °C) and tin (T_m = 231.88 °C) at a heating rate of 10 K/min. Furnace calibration was performed between 0 and 290 °C. For the dynamic measurements the samples were first heated at a rate of 40 K/min to a melt temperature of 260 °C, and kept there for 3 min in order to erase all thermal history. In one experiment this isothermal time was extended to 60 min. Then, the samples were cooled at 10 K/min to 25 °C. Subsequent melting scans were performed at a rate of 10 K/min. Sample masses of about 5 mg were used in case of scan rates of 10 K/min. Weighing was done using an AND Hm-202 balance with an accuracy of 0.01 mg. DSC curves were corrected for instrumental curvature by subtracting empty-pan curves, measured using identical thermal histories.

For the isothermal crystallization measurements the sample was heated at a rate of 40 K/min to a melt temperature of 260 °C, and kept there for 3 min, similar to the dynamic experiments. In the second step the sample was cooled down to the isothermal crystallization temperature T_{iso} at a rate of 10 K/min, followed by an isothermal period long enough to complete measurable crystallization of the material at the particular isothermal temperature. Subsequent melting after isothermal crystallization was performed at a heating rate of 10 K/min. A normal calibration set-up at 10 K/min heating rate was used for calibration but the isothermal temperature was each time set corresponding to the real sample (sensor) temperature (instead of the DSC program temperature). The crystallization half time was determined by calculating the time to reach 50% of the total area under the isothermal peak as a function of time. Glass transition temperatures of PS, (PPE/PS), SMA2, SMA17 and the (PPE/PS)/SMA17 50/50 w/w mixture were determined by using the first heating scan at a rate of 10 K/min.

2.5.2. Self-nucleation experiments

Self-nucleation experiments were also performed using the Pyris 1 DSC. With this method the nucleation density is increased enormously by heating up the material within the self-nucleation regimes where small crystal fragments are still present in the melt [35].

The following procedure was applied in this investigation:

Step 1 Erasing thermal history and creating a initial standard state. The samples were first heated to 260 °C at 40 K/min, and kept there for a 3 min isothermal period. Subsequently, the samples were cooled to room temperature at a cooling rate of 10 K/min.

Step 2 Heating to T_s (self nucleation temperature), situated between 220 and 260 °C, at a heating rate of 10 K/min. If T_s is 260 °C or higher, the sample is said to be in domain I, where complete melting is realized. When T_s is high enough to melt the material almost completely, but low enough to leave small crystal fragments capable of acting as self-nuclei, this is domain II, the self-nucleation region. When T_s is too low, only part of the crystals will be melted, and quite some remaining crystals will be annealed at T_s. This is domain III, giving rise to both self-nucleation and annealing.

Step 3 Isothermal conditioning at T_s during 3 minutes.

Step 4 Crystallization at a cooling rate of 10 K/min from T_s to room temperature.

Step 5 Melting after crystallization at a heating rate of 10 K/min.

2.6. Calculation of the number of heterogeneities

For the calculation of the number of heterogeneities it is assumed that the distribution of heterogeneities over the droplet population follows a Poisson distribution, analogue to the approximation of Pound and LaMer for the distribution of heterogeneities for monodisperse tin droplets [36]. Considering a large number of small polymer droplets, each having a volume V_D, the fraction of droplets that contain exactly z heterogeneities of type i that can nucleate the polymer can then be given by [16]:

$$f_z^i = \left[(M^i V_D)^z / z!\right] \exp(-M^i V_D) \tag{5}$$

where M^i is the concentration of heterogeneities of type i, and $M_i V_D$ is the mean number of heterogeneities per droplet with volume V_D.

The fraction of droplets, which contain at least one heterogeneity of type i is given by:

$$f_{z>0}^i = 1 - \exp(-M^i V_D) \tag{6}$$

or:

$$M^i = -[\ln(1 - f_{z>0}^i)]/V_D \tag{7}$$

This fraction can be calculated from the relative partial area of each crystallization exotherm during cooling in the DSC. On the assumption that one nucleus is sufficient to crystallize the whole droplet, calculations can be done with respect to the concentration of the respective heterogeneities, if the mean size of the droplets is known [16]. So for $i=1$, corresponding to the type of nuclei active at $T_{c(bulk)}$, one can calculate:

$$M^1 = -[\ln(1 - f_{z>0}^1)]/V_D \tag{8}$$

$$\text{in which } f_{z>0}^1 = \frac{\Delta h_c \text{ bulk}}{\Delta h_c \text{ total}} \tag{9}$$

and for the total number of heterogeneities ($i=1+2+3\ldots$) the following estimation was used:

$$M^{total} = \frac{-\ln(1 - f_{z>0}^{total})}{V_D} \tag{10}$$

with $f_{z>0}^{total}$ the fraction of droplets containing at least one heterogeneity of type $1+2+3\ldots$. $(1 - f_{z>0}^{total})$ is equal to the fraction of droplets crystallizing homogeneously (in the absence of heterogeneities). So, we can calculate the total number of heterogeneous nuclei via:

$$M^{total} = \frac{-\ln(\text{fraction homogeneous})}{V_D} \tag{11}$$

in which 'fraction homogeneous' $= \Delta h_c(T_{hom})/\Delta h_c$total.

3. Results and discussion

3.1. Effect of compatibilizer SMA2 on the dynamic and isothermal crystallization behavior of PA6

Before studying the effect of reactive compatibilization on the crystallization behavior of dispersed PA6 polymer droplets, the effect of the reactive compatibilizer on the bulk PA6 crystallization and its melting behavior was investigated. Binary blends of PA6 and SMA2 of different compositions were prepared using the DSM twin-screw extruder. Upon melt blending, a graft reaction takes place between the PA6 chain ends and the reactive modifier styrene-maleic anhydride copolymer, denoted by PA6-*g*-SMA. This is known to be a fast reaction between the maleic anhydride functionalities of SMA2 and the amine-end groups of PA6 [37]. The formation of the PA6-*g*-SMA graft copolymer during extrusion could be clearly indicated; the torque exerted on the screws showed a strong increase during melt mixing.

Fig. 1 shows the percentage of PA6 that has crystallized as a function of time for different extruded PA6/SMA2 mixtures at an isothermal crystallization temperature of 200 °C. In Fig. 2 the crystallization half-time $t_{1/2}$ is plotted for different isothermal crystallization temperatures in the temperature range 196–201 °C. As expected, the crystallization half-time decreases with decreasing temperature, which reflects the increasing overall rate of crystallization with decreasing temperature. The plot shows clearly that the addition of a small amount of compatibilizer SMA2 decreases the crystallization half-time, and thus increases the overall rate of crystallization. Addition of more SMA2, however, reduces the overall crystallization rate. Table 2 gives the values for T_c, Δh_c and Δh_m as calculated from DSC crystallization and melting experiments at 10 K/min for the different PA6/SMA2 compositions. These data are in line with the results from the isothermal experiments: at low SMA2 fractions small increases in Δh_c and Δh_m for PA6 are observed. At higher fractions T_c,T_m and Δh_c, Δh_m decrease

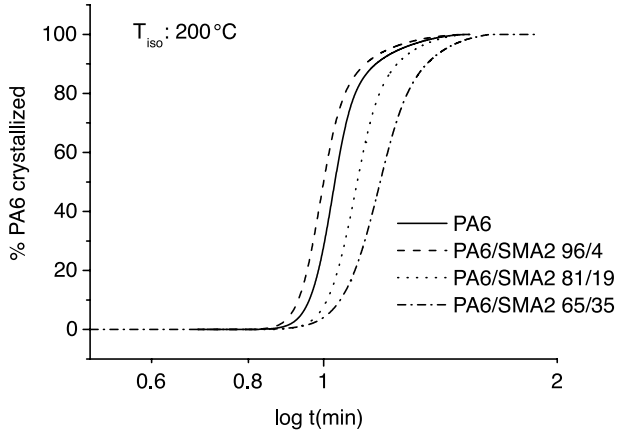

Fig. 1. Percentage PA6 crystallized as a function of log time at 200 °C for PA6 and PA6/SMA2 blends.

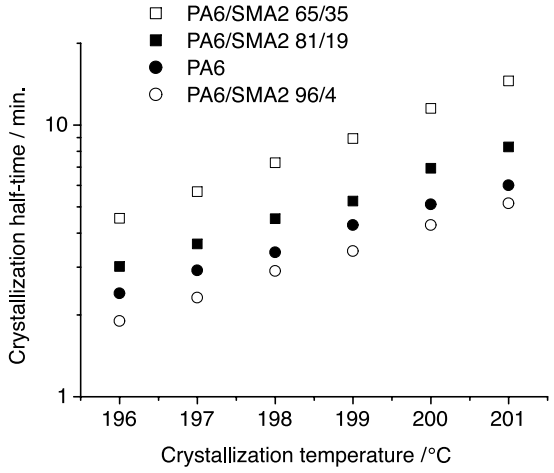

Fig. 2. Crystallization half-time as a function of crystallization temperature for PA6 and PA6/SMA2 blends.

significantly. The isothermal and dynamic DSC experiments thus point to a small nucleating effect of SMA2 when the amount of SMA2 reacted/blended with PA6 is low. Increasing the SMA2 concentration clearly disturbs the crystallization, leading to lower crystallization/melting temperatures and a decreased crystallinity.

Similar experimental observations have been done by other authors [37–39]. The disturbance of crystallization at higher concentrations is most likely related to reduced chain mobility, especially at high anhydride/amine ratios, resulting in slower crystallization. Van Duin et al. [37] observed a strongly reduced crystallinity at high anhydride/amine ratios. For a PA6/SMA20 50/50 w/w binary blend, even no crystallinity of PA6 could be observed at all at long mixing times [38].

3.2. Effect of reactive compatibilization on the crystallization behavior of dispersed PA6 droplets

3.2.1. Effect of low functionality SMA compatibilizer on the dynamic crystallization behavior of PS/PA6 and (PPE/PS)/PA6 blends

In Fig. 3 the DSC cooling curves are shown for different PS/PA6 and (PPE/PS)/PA6 blend compositions, which were reactively compatibilized with SMA2, according to mixing method 1 (see Section 2). The effects of the SMA2 compatibilizer on the phase morphology of PS/PA6 and (PPE/PS)/PA6 blend systems was published recently [34], in which it was concluded that SMA2 is a very effective compatibilizer for these blend systems. In Table 3 the morphological data are presented for the different SMA2 compatibilized PS/PA6 and (PPE/PS)/PA6 blend compositions varying the PA6 content, together with the crystallization data obtained with DSC. The PS/SMA2 ratio (mixing method 1) was always 92/8 w/w except indicated otherwise. For the blends where PA6 forms the matrix, or for blends with a co-continuous phase morphology,

Table 2
Thermal properties of PA6 and PA6/SMA2 binary blends

Blend system	PA6 (wt%)	$T_{c,peak}$ (°C)	Δh_c (J/g$_{PA6}$)	Δh_m (J/g$_{PA6}$)	$T_{m,peak}$ (°C)
PA6	100	188	77	81	221
PA6/SMA2	96	188	81	86	221
	81	185	55	65	220
	65	183	49	43	219

compatibilization with SMA2 results in a minor decrease in bulk crystallization temperature (from 188 to ~180 °C) as well as in crystallization and melting enthalpy. These effects can be mainly attributed to the disturbance of the SMA2 compatibilizer on the PA6 crystallization as explained in Section 3.1. As can be seen in Fig. 3, a very strong transition in crystallization behavior is observed when the blend morphology changes from a co-continuous phase morphology to a phase morphology with PA6 droplets. For instance, compare the crystallization behavior of (PS/SMA2)/PA6 55/45 having a co-continuous phase morphology to that of (PS/SMA2)/PA6 60/40, having PA6 droplets dispersed in PS matrix.

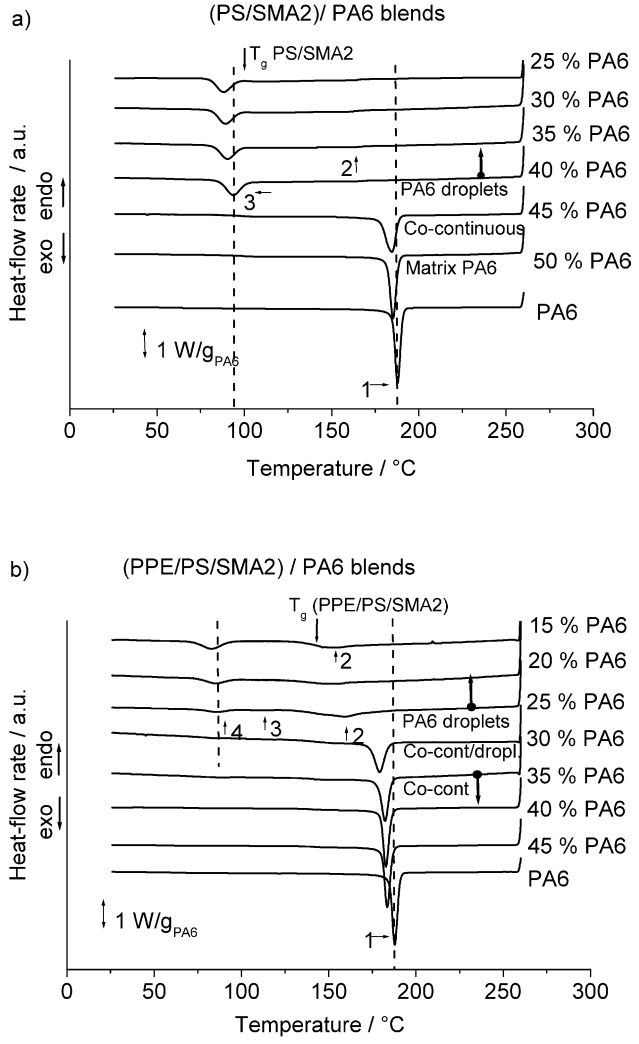

Fig. 3. DSC crystallization curves for different compositions of (a) (PS/SMA2)/PA6 blends and (b) (PPE/PS/SMA2)/PA6 blends. (PS/SMA2 ratio 92/8 w/w, (PPE/PS/SMA2)/PA6 80/20 and 85/15: 95/5 w/w (PPE/PS)/SMA2.

The changes in crystallization behavior when the polymer is dispersed in droplets were already discussed in part 1 of this paper series [21] for the uncompatibilized blends. The fractionated crystallization phenomenon in the uncompatibilized PS/PA6 and (PPE/PS)/PA6 blends induces up to 3 different crystallization peaks at higher supercoolings at the expense of crystallization around the bulk temperature. The degree of fractionated crystallization strongly depends on the size of the droplets and the droplet size distribution. Reactive compatibilization with SMA2 strongly decreases the PA6 droplet size in the blend systems by a factor of 10, from 1–2 to 0.1–0.2 μm on average. In addition, the droplets show a quite monodisperse droplet size distribution after compatibilization. As a result of the smaller size, the number of PA6 droplets per unit volume increases significantly. As can be seen in Fig. 3 reactive compatibilization induced an enormous retardation of the crystallization. The bulk crystallization around 188 °C (peak 1) is completely suppressed and a crystallization peak emerges around 85 °C (peak 3 Fig. 3a, peak 4 Fig. 3b), about 100 °C lower than the bulk crystallization temperature. Besides, a second crystallization peak is seen around 160 °C (peak 2), which is hardly discernable for the (PS/SMA2)/PA6 blends but is clearly observable for the (PPE/PS/SMA2)/PA6 blends.

In Fig. 4 the specific effect of the SMA2 compatibilizer

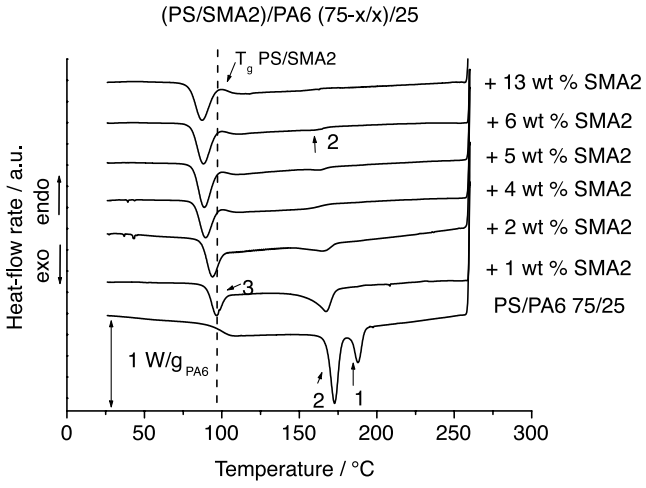

Fig. 4. DSC crystallization curves of (PS/SMA2)/PA6 75/25 blends with different SMA2 concentrations.

Table 3
Morphological and thermal parameters of (PS/SMA2)/PA6 and (PPE/PS/SMA2)/PA6 blend compositions

Blend system	PA6 (wt %)	D_n PA6 (μm)	(D_v/D_n) (–)	N_v (cm^{-3})	$T_{c,peak}$ (°C)				Δh_c (J/g_{PA6})				Δh_m (J/g_{PA6})	$T_{m,peak}$ (°C)
					1	2	3	4	1	2	3	4		
PA6	100	–	–	–	188	–	–	–	77	–	–	–	81	221
PS/SMA2/	15	–	–	–	–	–	–	–	–	–	–	–	–	–
PA6	20	–	–	–	–	–	–	–	–	–	–	–	–	–
	25	0.13	1.4	8.4×10^{13}	–	160	–	88	–	1	–	27	62	219
	30	0.15	1.4	5.7×10^{13}	–	156	–	89	–	5	–	28	58	219
	35	0.19	1.6	2.2×10^{13}	–	161	–	90	–	6	–	27	57	220
	40	0.29	1.9	5.1×10^{12}	–	162	–	94	–	4	–	30	58	219
	45	Co–cont	–	–	185	–	–	–	66	–	–	-	77	220
	50	Co-cont	–	–	185	–	–	–	70	–	–	–	79	220
PPE/PS/	15[a]	0.09	1.7	8.9×10^{13}	–	~150–160[b]	–	83	–	7[b]	–	25	56	218
SMA2/	20[a]	0.13	1.6	4.2×10^{13}	–	~150–160[b]	111	85	–	15[b]	1	13	53	218
PA6	25	0.17	1.8	1.1×10^{13}	–	~150–160[b]	111	85	–	36[b]	1	7	51	218
	30	Co-cont	–	–	179	–	–	84	45	–	–	2	61[c]	218
	35	Co-cont	–	–	181	–	–	85	54	–	–	2	64[c]	219
	40	Co-cont	–	–	183	–	–	–	58	–	–	–	67[c]	219
	45	Co-cont	–	–	184	–	–	–	58	–	–	–	70[c]	219

[a] (PPE/PS/SMA2) 95/5 w/w premixture.

[b] These crystallization peak positions could not be determined accurately due to overlap of the peaks with the glass transition of (PPE/PS) ($T_g \sim 150$ °C). Peak intensities as given were determined from the relative increase of the melting enthalpy before and after crystallizing this peak and by assuming that to formed crystals in this temperature region did not show extensive reorganization or recrystallization during heating [40].

[c] These data could be a little underestimated because of overlap of the onset of the melting peak with the glass transition of (PPE/PS).

on the droplet crystallization is displayed. This figure shows the crystallization curves of PS/PA6 75/25 blends, with increasing amounts of SMA2 compatibilizer, blended according to method 1: premixing SMA2 with PS. The morphological data are given in Table 4. The PS/PA6 without compatibilizer is characterized by two crystallization peaks, one at $T_{c,bulk}$ (188 °C) and the second around 170 °C, caused by fractionated crystallization in the uncompatibilized droplets having $D_n = 2$ μm [21]. Already at a very low concentration (1 wt% SMA2 on blend total) a significant effect on the size of the PA6 droplets is found, which immediately causes a strong shift of the crystallization peaks. A peak at low temperature is formed around 95 °C while the peaks at 188 and 170 °C decrease in intensity. As such, no significant nucleating effect of the SMA2 compatibilizer, as observed for low PA6/SMA2 ratio's (see Section 3.1), is seen, which could lead to a lower degree of fractionated crystallization. It is very likely that the high efficiency of the reactive compatibilizer, strongly reducing the droplet size even at relatively small concentrations, dominates over the possible nucleating effect of the small amount of copolymer formed at the interface. With increasing concentration of SMA2 the intensity of the low temperature peak in between 86 and 96 °C increases and the peaks at 188 °C (bulk) and in between 159 and 170 °C decrease in intensity. At high SMA2 concentrations (5.6 and 13 wt% SMA2) the decrease in droplet size tends to level off and the crystallization behavior is hardly affected anymore.

3.2.1.1. Comparison of the degree of fractionated crystallization for uncompatibilized and reactively compatibilized blend compositions. Fig. 5 shows an overview of the fractionated crystallization process as a function of the blend morphology for both uncompatibilized blends, discussed in part 1 [21], as well as for reactively

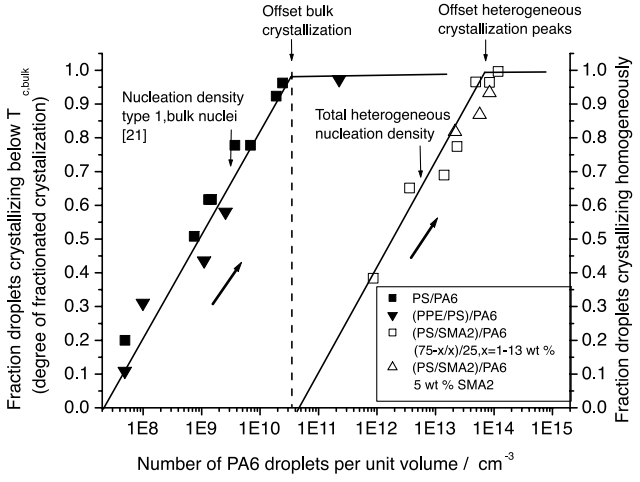

Fig. 5. Fraction of droplets crystallizing below $T_{c,bulk}$ (left *Y*-axis, closed data points) and homogeneously (right *Y*-axis, open data points) as a function of the number of PA6 droplets per unit volume for both uncompatibilized as SMA2 compatibilized PS/PA6 and (PPE/PS)/PA6 blends.

Table 4
Morphological and thermal parameters of (PS/SMA2)/PA6 75/25 and PS/(PA6/SMA2) 75 − *x*/(25/*x*) blends

Blend system	PA6 (wt %)	D_n PA6 (μm)	(D_v/D_n) (−)	N_v (cm^{-3})	$T_{c,peak}$ (°C)				Δh_c (J/g$_{PA6}$)				Δh_m (J/g$_{PA6}$)	$T_{m,peak}$ (°C)
					1	2	3	4	1	2	3	4		
PA6	–	–	–	–	188	–	–	–	77	–	–	–	81	221
PS/PA675/25														
First PS/SMA2	0	2.1	2.4	3.7×10^{9}	188	173	–	–	12	42	–	–	55	220
blending	1	0.59	1.4	8.6×10^{11}	188	167	–	96	0.1	24	–	13	56	220
	1.5	0.36	1.4	3.6×10^{12}	188	165	–	93	0.1	9	–	17	55	220
	3	0.24	1.3	1.4×10^{13}	–	165	–	90	–	8	–	23	56	220
	4	0.23	1.2	2.3×10^{13}	–	163	–	89	–	7	–	24	59	219
	5	0.17	1.3	4.9×10^{13}	–	163	–	88	–	1	–	28	59	219
	6	0.13	1.4	8.4×10^{13}	–	160	–	88	–	1	–	27	62	219
	13	0.11	1.5	1.2×10^{14}	–	159	–	86	–	0.1	–	29	61	218
First PA6/SMA2	1	1.28	1.6	5.4×10^{10}	187	170	–	–	10	41	–	–	55	219
blending	6	0.74	1.8	2.0×10^{11}	185	166	–	102	2	32	–	3	60	219
	13	0.68	1.8	2.5×10^{11}	184	150	119	99	1	12	2	6	58	217

compatibilized blends. Different (PS/SMA2)/PA6 blend compositions are displayed, each containing about 5 wt% compatibilizer SMA2 (data of Fig. 3). Also, (PS/SMA2)PA6 (75−*x*/*x*)/25 blends are plotted with *x*, the SMA2 concentration, ranging from 1 to 13 wt% (data of Fig. 4). The number of PA6 droplets on the *X*-axis was calculated using a volume average droplet diameter. On the *Y*-axis two different values for the degree of fractionated crystallization have been indicated (left and right axis). The left *Y*-axis corresponds to the closed data points related to the uncompatibilized PS/PA6 and (PPE/PS) blends, and shows the fraction of PA6 droplets crystallizing below the bulk nucleation peak. The right *Y*-axis corresponds to the open data points, related to the compatibilized blends, and displays the fraction of droplets crystallizing at the lowest crystallization temperature (~85 °C).

This figure can be interpreted in the following way: by increasing the number of droplets per unit volume via decreasing the droplet size, fractionated crystallization becomes more pronounced and the fraction of droplets that crystallizes at lower temperatures by nuclei of lower activity increases. With increasing number of droplets per unit volume, the fraction of droplets crystallized by nuclei of type 2, 3 etc. is increased and the fraction of droplets crystallized by type 1 nuclei at $T_{c,bulk}$ decreases. In part 1 [21] the number of heterogeneities active at the bulk temperature was calculated according to Eq. (8), assuming a Poisson distribution of nuclei over the droplet population with an average droplet volume. A nucleation density of bulk nuclei of approximately 1×10^{9}–1×10^{10} cm^{-3} could be calculated. Upon reactive compatibilization, however, the PA6 droplet size is further decreased. At some point then, also the heterogeneous nuclei with a lower activity are exhausted and nucleation can only take place homogeneously via self-association of the PA6 chains. This can be expected to take place at the lowest crystallization temperature observed. The evolution of the homogeneous nucleation peak is plotted on the right *Y*-axis. For this, the relative area under the crystallization peak with the highest observed supercooling (T_c=85–90 °C) was taken, corresponding to the fraction of droplets crystallizing at this temperature. It is shown in a forthcoming paper [41] by studying the crystallization kinetics, that the droplets crystallizing at this low temperature are indeed most likely nucleated via a homogeneous nucleation mechanism. It can be seen that the area of the homogeneous nucleation peak is increasing with increasing number of droplets (1×10^{11} to 1×10^{14}) until finally the biggest part of the material crystallizes homogeneously (>97%). Interestingly the onset for homogeneous nucleation seems to coincide with the offset of the bulk crystallization, around 5×10^{10} number of droplets per unit volume.

For calculating the total number of heterogeneous nuclei (type 1+2+3…) we can use Eq. (10). Calculating the average volume of the droplets by using the volume average droplet diameters (via data in Tables 3 and 4), we obtain: $M^{total}\sim6\times10^{12}$ nuclei/cm^3, indicated in Fig. 5. The other arrow at around 6×10^{9} nuclei/cm^3 indicates the number of heterogeneities of type 1 ($T_{c,bulk}$ nuclei), as determined in [21]. The two lines plotted through the data points, indicated in Fig. 5, thus represent the evolution of different crystallization peaks of heterogeneous origin for numbers of droplets between 1×10^{7} and 1×10^{11} per cm^3 in the uncompatibilized blends, followed by the evolution of the crystallization of homogeneous origin at bigger numbers of droplets per unit volume (1×10^{11}–1×10^{14} cm^{-3}), induced by reactive compatibilization. The different (PS/SMA2)PA6 blend compositions with 5 wt% SMA2 clearly follow the same trend as the PS/PA6 75/25 blend with varying SMA2 concentration. Because similar degrees of homogeneous nucleation are reached for comparable number of droplets per unit volume, irrespective of the amount of SMA2 compatibilizer added, the fractionated crystallization upon reactive compatibilization thus seems to be mainly determined by the decrease in PA6 droplet size.

3.2.1.2. Effect of the mixing method of the SMA2 compatibilizer on the fractionated crystallization process. Fig. 6 shows the crystallization behavior of PS/PA6 75/25 blends, but in this case the SMA2 compatibilizer was first premixed with PA6 (mixing method 2), leading to the formation of PA6-SMA2 grafted chains inside the PA6 phase. To become effective the PA6-*g*-SMA2 chains have to diffuse towards the PS interface in the second blending step with PS. The morphological data of both blend series presented in Table 4, show that the morphology of the PA6/SMA2 premixed blends is much coarser than that generated after premixing PS/SMA2 (method 1). The droplet size is reduced to about 0.7 μm for the PA6/SMA2 premixed blend, compared to about 0.1 μm for the PS/SMA2 premixed blend, which is reached after addition of 6 wt% of SMA2. Increasing the SMA2 concentration up to 13 wt% has hardly any further effect on the morphology.

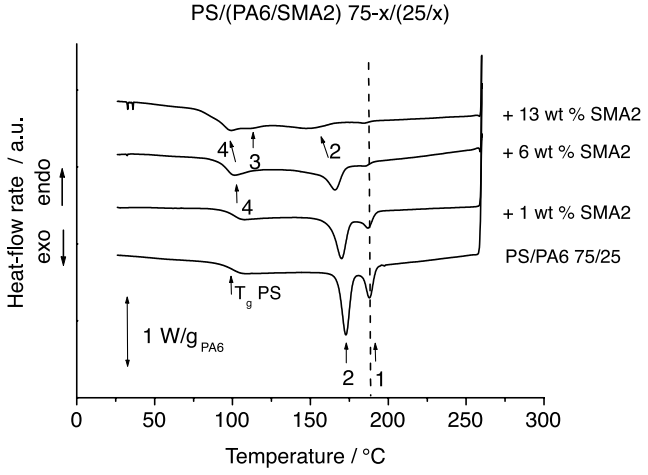

Fig. 6. DSC crystallization curves of (PS/(PA6/SMA2) 75−*x*/(25/*x*) blends with different SMA2 concentrations.

Although the crystallization behavior of the PA6 droplets shows the same general trends as with mixing method 1—an increase in number and intensity of the low temperature peaks and parallel decrease of the bulk crystallization peak with decreasing PA6 droplet size- an interesting observation can be made. As can be seen from Fig. 6, increasing the amount of SMA2 from 6 to 13 wt%, having hardly any effect on the morphology anymore (Table 4), still leads to a shift towards crystallization at the lowest crystallization temperatures. However, at the same time, the crystallization peak areas decrease significantly. Most probably this is due to the reaction of the excess anhydride groups with the PA6 amide groups. As a result of this, the number of PA6 chains available for crystallization is decreased drastically, while crystallizable PA6 chains will be hindered in crystallization. This too can cause fractionated crystallization.

3.2.1.3. Effect of the matrix interface on fractionated crystallization. Fig. 7 again shows the fractionated crystallization as a function of the number of droplets but now the compatibilized (PPE/PS/SMA2)/PA6 blend compositions have been included in the graph (preparation via mixing method 1). The efficiency of the compatibilization in reducing the droplet size of the (PPE/PS)/PA6 blends is confirmed by the large number of PA6 droplets per unit volume obtained after reactive compatibilization ($\sim 1\times 10^{13}$–1×10^{14} cm^{-3}). However, for these blends a significant lower fraction of the PA6 droplets crystallizes at the homogeneous nucleation temperature for equal number of droplets per unit volume, compared to the (PS/SMA2)/PA6 blends. Using Eq. (10), a total nucleation density of $\sim 1.5\times 10^{14}$ nuclei/cm^3 for the (PPE/PS/SMA2)/PA6 blends is calculated, compared to $\sim 6\times 10^{12}$ nuclei/cm^3 for the (PS/SMA2)/PA6 blends. In a previous publication [21] it was shown that a nucleating activity of the matrix interface was found when the matrix phase vitrified before the crystallization of the dispersed PA6 phase started. The (PPE/PS 50/50) matrix considered here has a T_g of about 150 °C. This transition partly overlaps with the fractionated crystallization peak found around 150–160 °C (see Table 3). As such, it is very likely that the vitrifying (PPE/PS) matrix interface will induce nuclei at this crystallization temperature. This leads to an enhancement of the total heterogeneous nucleation density and a lower relative amount of crystallization at the highest supercooling. It can also be concluded that the miscible SMA2 compatibilizer present at the interface apparently does not seem to affect the nucleation behavior of the amorphous matrix phase towards the PA6 droplets.

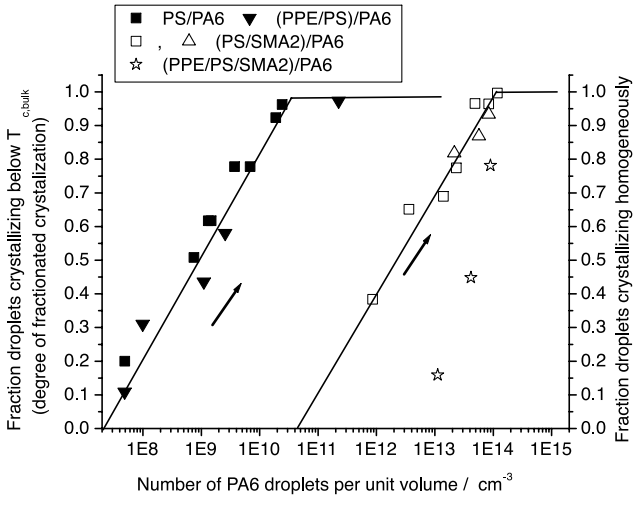

Fig. 7. Fraction of droplets crystallizing below $T_{c,bulk}$ (left *Y*-axis) or homogeneously (right *Y*-axis) as a function of number of PA6 droplets per unit volume for uncompatibilized and SMA2 compatibilized PS/PA6 and (PPE/PS)/PA6 blend compositions.

3.2.2. Effect of high functionality SMA compatibilizer on the dynamic crystallization behavior of PA6 droplets dispersed in PPE/PS matrix

A number of (PPE/PS)/PA6 blends were also reactively compatibilized using SMA17 instead of SMA2. From literature data it is known that blends of PS and SMA are only miscible up to MA concentrations in SMA of 3 wt%. For PPE the miscibility with SMA is increased up to about 8 wt% of MA [32,33]. It is thus expected that (PPE/PS) 50/50 is miscible with SMA2, but immiscible with SMA17. To verify this, the glass transition temperatures of these two binary blends have been determined using DSC as indicated in Fig. 8. Indeed, for the (PPE./PS) 50/50 /SMA17 mixture, two transitions can be observed, compared to a single transition for the SMA2 blend, which clearly indicates immiscibility. A clear separation of the two T_g's, having the same values as the pure components, is however not obtained. This probably points to a partial miscibility of the 50/50 w/w mixture for the applied blend conditions. Fig. 9 shows the volume average droplet diameter D_v of PA6 droplets for different (PPE/PS)/PA6 blend compositions, with and without compatibilizers SMA2 and SMA17. For compatibilization the SMA17 compatibilizer was first premixed with (PPE/PS), similar to the blend experiments

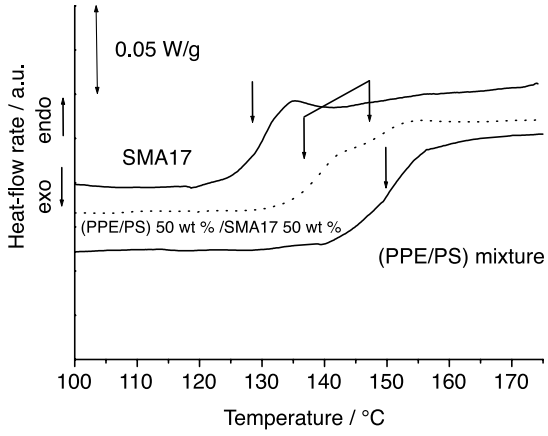

Fig. 8. DSC heating curves at 10 K/min of (PPE/PS) 50/50 mixture, SMA17 and (PPE/PS) 50 wt%/SMA17 50 wt% blend.

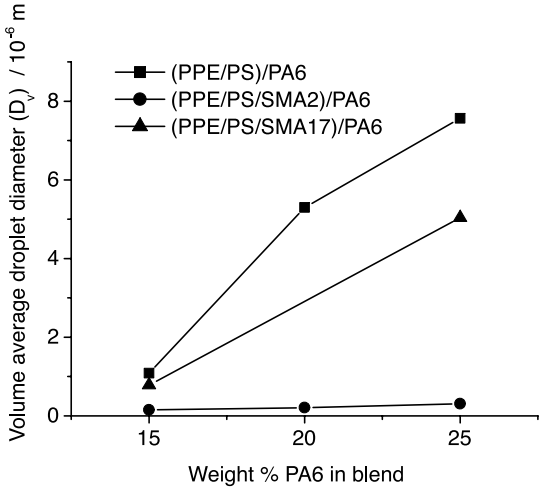

Fig. 9. Volume average droplet diameter versus blend composition for (PPE/PS)/PA6, (PPE/PS/SMA2)/PA6 and (PPE/PS/SMA17)/PA6 blend compositions.

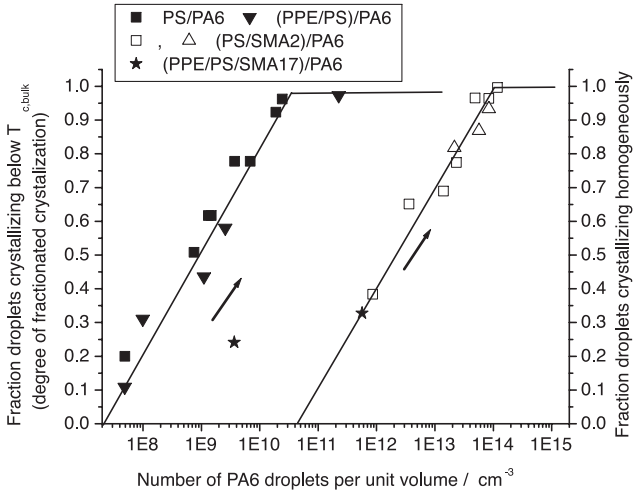

Fig. 10. Fraction of droplets crystallizing below $T_{c,bulk}$ (left *Y*-axis, closed data points) or homogeneously (right *Y*-axis, open data points) as a function of number of PA6 droplets per unit volume for uncompatibilized and SMA2 and SMA17 compatibilized PS/PA6 and (PPE/PS)/PA6 blend compositions.

with the SMA2 compatibilizer (mixing method 1). The data clearly show that SMA17 is a much less efficient compatibilizer for the (PPE/PS)/PA6 blends, compared to SMA2. The PA6 droplet diameter is decreased only a little bit upon compatibilization. The strong increase of the torque, observed during melt-mixing, however, does indicate the formation of grafted polymer chains. The tendency of the components SMA17 and (PPE/PS 50/50) to demix, as could be concluded from the T_g determinations, can result in the formation of an immiscible interlayer of (PPE/PS/SMA17-*g*-PA6) between the (PPE/PS) and PA6 blend components or even causing the interfacially formed graft copolymer SMA17-*g*-PA6 to migrate towards the PA6 phase [42]. These phenomena can possibly explain the strongly reduced compatibilization efficiency for the (PPE/PS/SMA17)/PA6 blends.

Fig. 10 again shows the fractionated crystallization as a function of the number of droplets per unit volume but now (PPE/PS/SMA17)/PA6 75/25 and 85/15 blend compositions have been inserted. The morphological and crystallization parameters for these two blend compositions are given in Table 5. The lower compatibilization efficiency of SMA17 is clearly visible, because the compatibilized (PPE/PS/SMA17)/PA6 blend compositions lead to relatively small number of PA6 droplets per unit volume compared to the SMA2 compatibilized blends. The plotted data points correspond to the left *Y*-axis, showing the fraction of droplets crystallizing below $T_{c,bulk}$. The degree of fractionated crystallization is much less for the (PPE/PS/SMA17)/PA6 compatibilized blends compared to the uncompatibilized PS/PA6 and (PPE/PS)/PA6 blends, at equal number of PA6 droplets per unit volume. As such, the presence of SMA17 seems to have caused an increase in nucleation density of type 1 crystallizing at the bulk crystallization temperature of PA6, leading to a lower degree of fractionated crystallization. Most likely the nucleation phenomena between the blend components (migration of impurities, interface nucleation) were affected by the change in interface type between the two components.

3.3. Nucleation experiments

The DSC curves in Figs. 3 and 4 show that for blends containing a very large number of PA6 droplets per unit volume, crystallization takes place predominantly at the homogeneous nucleation temperature. It can be expected that when the nucleation density in the dispersed droplets is increased significantly, the relative amount of heterogeneous bulk nucleation will increase. To enhance the heterogeneous nucleation density in the droplets, two different kinds of nucleation experiments were performed. The first method is self-nucleation. In the second method talc powder has been added as nucleating agent for PA6.

3.3.1. Self-nucleation experiments

In Fig. 11 the DSC crystallization and melting curves obtained after applying the self-nucleation procedure are presented for a (PS/SMA2)/PA6 (62/13)/25 blend. Self-nucleation experiments provide an easy way to increase the nucleation density of a semicrystalline polymer, by leaving small crystal fragments in the molten state prior to crystallization. Up to a premelting temperature T_s of about 228 °C the crystallization behavior of the PA6 droplets in the blend remains unaffected and a single homogeneous crystallization peak is observed at about 85 °C. Lowering the premelting temperature T_s into the self-nucleation regime, results in a strong increase of the amount of nuclei and reintroduces heterogeneous bulk nucleation in the 100 nm domains around 188 °C. Finally, at a heating

Table 5
Morphological and thermal parameters of PA6/SMA17, (PPE/PS)/PA6 and (PPE/PS/SMA17)/PA6 blend compositions

Blend system	PA6 (wt %)	D_n PA6 (μm)	(D_v/D_n) (–)	N_v (cm^{-3})	$T_{c,peak}$ (°C)				Δh_c (J/g_{PA6})				Δh_m (J/g_{PA6})	$T_{m,peak}$ (°C)
					1	2	3	4	1	2	3	4		
PA6ex	100	–	–	–	189	–	–	–	77		–	–	81	221
PA6/SMA17	81	–	–	–	183	–	–	–	59		–	–	64	218
PPE/PS/	15	0.35	3.1	2.2×10^{11}	187	162	–	89	1	36	–	<1	49	220
PA6	25	0.61	12.4	1.1×10^{9}	187	~160[a]	113	–	22	12[a]	5	–	60	220
PPE/PS/	15	0.46	1.7	5.6×10^{11}	185	~160[a]	–	89	39	18[a]	–	1	56	218
SMA17/	25	2.4	2.1	3.7×10^{9}	183	~160[a]	–	–	44	14[a]	–	–	59	217
PA6														

[a] These crystallization peak positions could not be determined accurately due to overlap of the peaks with the glass transition of (PPE/PS) (T_g ~ 150 °C). Peak intensities as given were determined from the relative increase of the melting enthalpy before and after crystallizing this peak and by assuming that to formed crystals in this temperature region did not show extensive reorganization or recrystallization during heating [40].

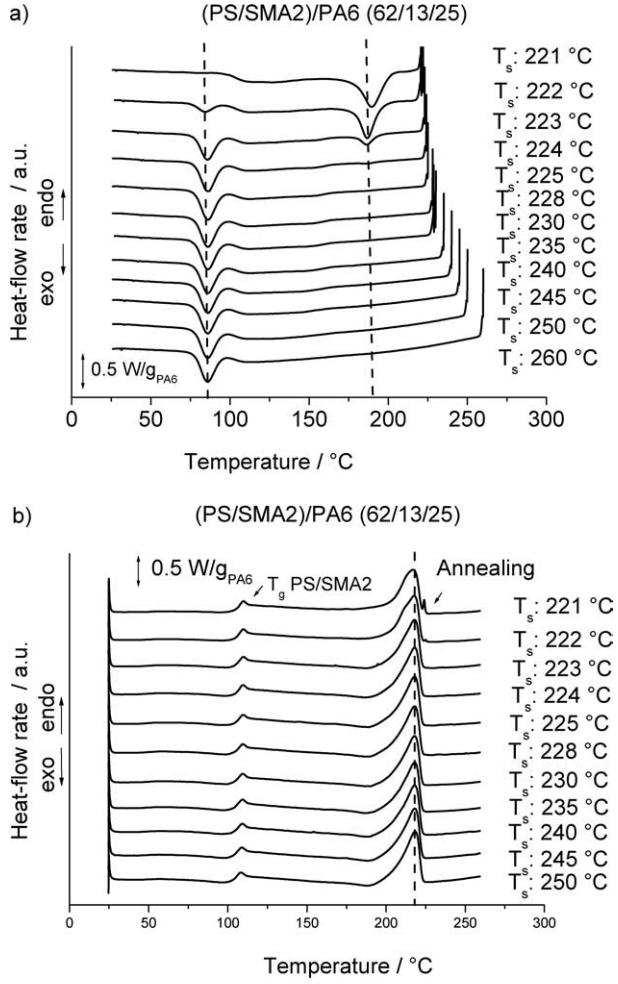

Fig. 11. Self-nucleation experiments for (PS/SMA2)/PA6 (62/13)/25, (a) DSC crystallization curves after different T_s, cooling rate: 10 K/min, (b) DSC melting curves at 10 K/min after crystallization from T_s.

temperature of 221 °C, all the material crystallizes at the bulk temperature. From the DSC melting curves it can be concluded that for these blend samples the temperature has to be decreased into the annealing domain of PA6 to achieve a complete nucleation of the droplets. This follows from the high temperature annealing peak around 225 °C in the subsequent heating scan to 260 °C for the samples heated to 221 °C and lower. The vertical, interrupted line drawn in Fig. 11a shows the effect of nucleation on the position of the crystallization peaks. With respect to temperature, the bulk peak representing heterogeneous nucleation, enforced by self-nucleation, shows an increase. Furthermore, it can be observed that the area of the melting peak for the material crystallizing at low temperature via homogeneous nucleation (T_s: 250 °C) is not reduced compared to the melting peak after self-nucleation (T_s, 221 °C). The final melting temperatures (interrupted line in Fig. 11b) are also the same, although the crystals are formed in different temperature intervals.

3.3.2. Addition of talc powder as nucleating agent

It is known that fine-sized talc powder can be a very effective nucleating agent for PA6. Fig. 12 shows the DSC crystallization curves of PA6, PS/PA6 75/25 and (PS/SMA2)/PA6 (69/6)/25 blends without and with addition of talc powder. For the compatibilized blend two different talc concentrations (0.5 and 2 wt%) were used. The size of the talc droplets was estimated (using optical microscopy) to be in the range of 0.1–1 μm. The morphology of the blends was not altered upon addition of talc powder. As expected, PA6 is effectively nucleated by the talc powder, resulting in an increase of the crystallization temperature (from 188 to 193 °C). The melting enthalpy is not significantly increased. The uncompatibilized PS/PA6 blend, having an average PA6 droplet size D_n of about 1.5 μm, is also effectively nucleated, causing a complete suppression of the fractionated crystallization. However, this is not the case for the reactively compatibilized blend, having an average PA6 droplet size of 100–150 nm. Just a little decrease of the amount of material crystallizing according to homogeneous nucleation is achieved in case of 0.5 wt% of talc. Addition of extra talc to 2 wt%, causes a further decrease of intensity of the homogeneous peak and a slight increase of the intensity of the bulk crystallization peak. Remarkably, though it is hardly seen in the figure, also the peak around 150 °C seems to be increased slightly upon addition of talc. The talc experiments clearly show that the nucleation density within the droplets can be enhanced, though it is obvious that—in order to prevent homogeneous nucleation—there is a real need for nucleating agents that are small enough to be well incorporated in the small droplets.

The above nucleation experiments clearly show that there is no physical restriction for crystallization in the submicrometer sized PA6 droplets: obviously though the crystallizable PA6 chains are confined to the submicrometer droplet dimensions, they are not hindered in crystallization by that.

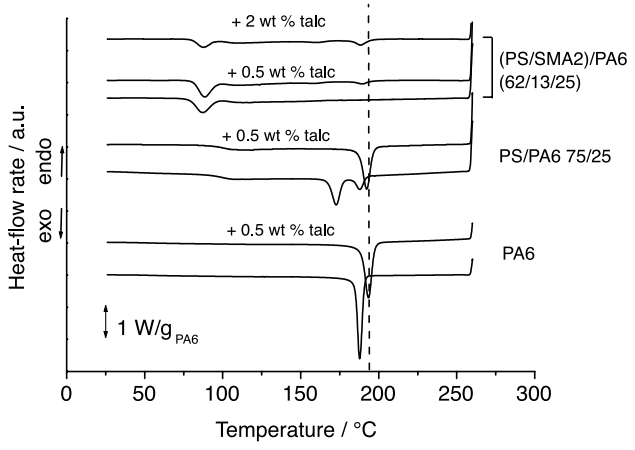

Fig. 12. DSC crystallization curves of PA6, PS/PA6 75/25 and (PS/SMA2)/PA6 (62/13)/25 blends, without and with talc nucleating agent.

4. Conclusions

Reactive compatibilization using a miscible compatibilizer (SMA2) allows excellent control of the PS/PA6 and (PPE/PS)/PA6 blend phase morphologies, resulting in a systematic decrease of the PA6 droplet size down to 100–150 nm with increasing compatibilizer concentration. The use of an immiscible compatibilizer (SMA17) leads to less efficient compatibilization. In this paper it has been shown that reactive compatibilization of PS/PA6 or (PPE/PS)/PA6 blends with SMA2 significantly affects the crystallization behavior of dispersed PA6 droplets. Fractionated crystallization is strongly enhanced in the submicron- sized PA6 droplets, leading to a delay of crystallization to very high supercoolings and ultimately to crystallization at temperatures as low as approximately 85 °C. A clear relation between the number of dispersed PA6 droplets per unit volume and the intensity of the homogeneous nucleation peak at this very low PA6 crystallization temperature has been found. There is little evidence for direct nucleation effects of the compatibilizer, though binary blends of PA6 and SMA2 showed a nucleating effect of SMA2 at low concentrations. Abundant reaction of the SMA2 compatibilizer with PA6 seems to reduce the mobility of PA6 chain segments, leading to an increased fractionated crystallization in the PA6 droplets. The importance of the interface governing the droplet crystallization phenomena has been clearly indicated. Both the matrix phase as well as presence of the compatibilizer at the droplet/matrix interface can alter the heterogeneous nucleation density. Vitrification of the matrix phase probably induces an extra amount of nuclei reducing fractionated crystallization. Reactive compatibilization of the blends with the (partly) immiscible compatibilizer SMA17 strongly lowers the degree of fractionated crystallization, when comparing similar droplet morphologies. Nucleation experiments show that homogeneous nucleation at very low crystallization temperature can be converted into heterogeneous bulk nucleation upon addition of enough nuclei of sufficient small size, indicating that also in the confined volumes of the droplets the lack of heterogeneities is the primary reason for the low temperature crystallization.

References

[1] Cormia RL, Price FP, Turnbull D. J Chem Phys 1962;37(6):1333.
[2] Burns JR, Turnbull D. J Appl Phys 1966;37(11):4021.
[3] Koutsky JA, Walton AG, Baer E. J Appl Phys 1967;38(4):1832.
[4] Gornick F, Ross GS, Frolen LJ. ACS Polym Prepr, Div Polym Chem 1966;7:82.
[5] Barham PJ, Jarvis DA, Keller A. J Polym Sci Phys Ed 1982;20:1733.
[6] Lotz B, Kovacs AJ. ACS Polym Prepr, Div Polym Chem 1969;10(2):820.
[7] O'Malley JJ, Crystal RG, Erhardt PF. ACS Polym Prepr, Div Polym Chem 1969;10(2):796.
[8] Robitaille C, Prudhomme J. Macromolecules 1983;16:665.

[9] Loo Y-L, Register RA, Ryan AJ. Phys Rev Lett 2000;84(18):4120.
[10] Loo Y-L, Register RA, Ryan AJ, Dee GT. Macromolecules 2001;34: 8968.
[11] Xu J-T, Fairclough PA, Mai S-M, Ryan AJ, Chaibundit C. Macromolecules 2002;35:6937.
[12] Lee W, Chen HL, Lin TL. J Polym Sci Part B: Polym Phys 2002; 40(6):519.
[13] Müller AJ, Balsamo V, Arnal ML, Jakob T, Schmalz H, Abetz V. Macromolecules 2002;35(8):3048.
[14] Müller AJ, Arnal ML, Lopez-Carrasquero F. Macromol Symp 2002; 183:199.
[15] Reiter G, Castelein G, Sommer J-U, Röttele A, Thurn-Albrecht T. Phys Rev Lett 2001;87(22) art no: 226101.
[16] Frensch H, Harnischfeger P, Jungnickel BJ. In: Utracki LA, Weiss RA, editors. Multiphase polymers: blends and ionomers. ACS Symp Series, vol. 395, 1989. p. 101.
[17] Santana OO, Müller AJ. Polym Bull 1994;32(4):471.
[18] Arnal ML, Matos ME, Morales RA, Santana OO, Müller AJ. Macromol Chem Phys 1998;199(10):2275.
[19] Everaert V, Groeninckx G, Aerts L. Polymer 2000;41:1409.
[20] Groeninckx G, Vanneste M, Everaert V. In: Utracki LA, editor. Polymer blends handbook. Crystallization, morphological structure and melting of polymer blends, vol. 1. Dordrecht: Kluwer Academic Publishers; 2002. p. 203–94. Chapter 3.
[21] Tol RT, Mathot VBF, Groeninckx G. Confined crystallization phenomena in immiscible polymer blends with dispersed micro and nanometer sized PA6 droplets. Part 1: uncompatibilized PS/PA6, (PPE/PS)/PA6 and (PPE/PA6) blends, this issue; 2004.
[22] Bartczak Z, Galeski A, Krasnikova NP. Polymer 1987;28:1627.
[23] Wenig W, Fiedel HW, Scholl A. Colloid Polym Sci 1990;268:528.
[24] Long Y, Stachurski ZH, Shanks RA. Polym Int 1991;26:143.
[25] Ikkala OT, Holsti-Miettinen RM, Seppälä J. J Appl Polym Sci 1993; 49:1165.
[26] Tang T, Huang B. J Polym Sci Part B: Polym Phys 1994;32:1991.
[27] Moon HS, Ryoo BK, Park JK. J Appl Polym Sci, Part B, Polym Phys 1994;32:1427.
[28] Mischenko N, Groeninckx G, Reynaers H, Koch M, Pracella M. Abstracts of the Fourth AIM Conference on Advanced Topics in Polymer Science 1996. Pisa, Italy.
[29] Psarski M, Pracella M, Galeski A. Polymer 2000;41:4923.
[30] Sanchez A, Rosales C, Laredo E, Müller AJ, Pracella M. Makromol Chem Phys 2001;202:2461.
[31] Everaert V, Groeninckx G, Pionteck J, Favis BD, Aerts L, Moldenaers P, Mewis J. Polymer 2000;41:1011.
[32] Fried JR, Hanna GA. Polym Eng Sci 1982;22:705.
[33] Witteler H, Leiser G, Drosher M. Makromol Chem Rapid Commun 1993;14:401.
[34] Tol RT, Groeninckx G, Vinckier I, Moldenaers P, Mewis J. Polymer 2004;45(8):2587–601.
[35] Blundell DJ, Keller A, Kovacs AJ. J Polym Sci 1966;B(4):481.
[36] Pound GM, LaMer VK. J Am Chem Soc 1952;74:2323.
[37] Van Duin M, Aussems M, Borggreve RJM. J Appl Polym Sci Part A: Polym Chem 1998;36(1):179.
[38] Van Duin M, Borggreve RJM. Reactive modifiers for polymers. In: Al-Malaika S, editor. Blends of polyamides and maleic-anhydride containing polymers: interfacial chemistry and properties. London: Chapman and Hall; 1997. Chapter 3.
[39] Kim BK, Park SJ. J Appl Polym Sci 1991;43:357.
[40] Tol RT, Mathot VBF, H. Reynaers, Groeninckx G. Confined crystallization phenomena in immiscible polymer blends with dispersed micro and nanometer sized PA6 droplets. Part 4: polymorphous structure and (meta)-stability of PA6 crystals formed in different temperature regions, submitted for publication; 2004.
[41] Tol RT, Mathot VBF, Groeninckx G. Confined crystallization phenomena in immiscible polymer blends with dispersed micro and nanometer sized PA6 droplets. Part 3: crystallization kinetics and crystallinity of micro and nanometer sized PA6 droplets crystallizing at very high supercoolings, submitted for publication; 2004.
[42] Majumdar B, Keskkula H, Paul DR, Harvey NG. Polymer 1994;35: 4263.